

REPORT DOCUMENTATION PAGE			Form Approved OMB NO. 0704-0188		
<p>The public reporting burden for this collection of information is estimated to average 1 hour per response, including the time for reviewing instructions, searching existing data sources, gathering and maintaining the data needed, and completing and reviewing the collection of information. Send comments regarding this burden estimate or any other aspect of this collection of information, including suggestions for reducing this burden, to Washington Headquarters Services, Directorate for Information Operations and Reports, 1215 Jefferson Davis Highway, Suite 1204, Arlington VA, 22202-4302. Respondents should be aware that notwithstanding any other provision of law, no person shall be subject to any penalty for failing to comply with a collection of information if it does not display a currently valid OMB control number.</p> <p>PLEASE DO NOT RETURN YOUR FORM TO THE ABOVE ADDRESS.</p>					
1. REPORT DATE (DD-MM-YYYY) 06-10-2014		2. REPORT TYPE Final Report		3. DATES COVERED (From - To) 1-Jun-2011 - 31-May-2014	
4. TITLE AND SUBTITLE Final Report: Combined Investigation on Durability and Dynamic Failure of Advanced Naval Materials			5a. CONTRACT NUMBER W911NF-11-1-0211		
			5b. GRANT NUMBER		
			5c. PROGRAM ELEMENT NUMBER 206022		
6. AUTHORS Jack Chessa			5d. PROJECT NUMBER		
			5e. TASK NUMBER		
			5f. WORK UNIT NUMBER		
7. PERFORMING ORGANIZATION NAMES AND ADDRESSES University of Texas at El Paso 500 West University Avenue El Paso, TX 79968 -0587			8. PERFORMING ORGANIZATION REPORT NUMBER		
9. SPONSORING/MONITORING AGENCY NAME(S) AND ADDRESS (ES) U.S. Army Research Office P.O. Box 12211 Research Triangle Park, NC 27709-2211			10. SPONSOR/MONITOR'S ACRONYM(S) ARO		
			11. SPONSOR/MONITOR'S REPORT NUMBER(S) 58987-MS-REP.3		
12. DISTRIBUTION AVAILABILITY STATEMENT Approved for Public Release; Distribution Unlimited					
13. SUPPLEMENTARY NOTES The views, opinions and/or findings contained in this report are those of the author(s) and should not be construed as an official Department of the Army position, policy or decision, unless so designated by other documentation.					
14. ABSTRACT The report					
15. SUBJECT TERMS Composites, Seawater, Fracture					
16. SECURITY CLASSIFICATION OF:			17. LIMITATION OF ABSTRACT UU	15. NUMBER OF PAGES	19a. NAME OF RESPONSIBLE PERSON Jack Chessa
a. REPORT UU	b. ABSTRACT UU	c. THIS PAGE UU			19b. TELEPHONE NUMBER 915-747-6900

Report Title

Final Report: Combined Investigation on Durability and Dynamic Failure of Advanced Naval Materials

ABSTRACT

The report

Enter List of papers submitted or published that acknowledge ARO support from the start of the project to the date of this printing. List the papers, including journal references, in the following categories:

(a) Papers published in peer-reviewed journals (N/A for none)

Received

Paper

07/25/2012	2.00	V. -X. Tran, D. Leguillon, A. Krishnan, L. R. Xu. Interface crack initiation at V-notches along adhesive bonding in weakly bonded polymers subjected to mixed-mode loading, International Journal of Fracture, (6 2012): 0. doi: 10.1007/s10704-012-9727-x
07/26/2012	1.00	L. Roy Xu, Arun Krishnan. A Simple Effective Flaw Model on Analyzing the Nanofiller Agglomeration Effect of Nanocomposite Materials, Journal of Nanomaterials, (02 2012): 0. doi: 10.1155/2012/483093

TOTAL: 2

Number of Papers published in peer-reviewed journals:

(b) Papers published in non-peer-reviewed journals (N/A for none)

Received

Paper

TOTAL:

Number of Papers published in non peer-reviewed journals:

(c) Presentations

Number of Presentations: 0.00

Non Peer-Reviewed Conference Proceeding publications (other than abstracts):

Received Paper

TOTAL:

Number of Non Peer-Reviewed Conference Proceeding publications (other than abstracts):

Peer-Reviewed Conference Proceeding publications (other than abstracts):

Received Paper

TOTAL:

Number of Peer-Reviewed Conference Proceeding publications (other than abstracts):

(d) Manuscripts

Received Paper

TOTAL:

Number of Manuscripts:

Books

Received Book

TOTAL:

TOTAL:

Patents Submitted

Patents Awarded

Awards

Graduate Students

NAME	PERCENT SUPPORTED	Discipline
Mr Mark Flores	0.75	
FTE Equivalent:	0.75	
Total Number:	1	

Names of Post Doctorates

NAME	PERCENT SUPPORTED
FTE Equivalent:	
Total Number:	

Names of Faculty Supported

NAME	PERCENT SUPPORTED	National Academy Member
Jack Chessa	0.08	
FTE Equivalent:	0.08	
Total Number:	1	

Names of Under Graduate students supported

NAME	PERCENT SUPPORTED
FTE Equivalent:	
Total Number:	

Student Metrics

This section only applies to graduating undergraduates supported by this agreement in this reporting period

The number of undergraduates funded by this agreement who graduated during this period: 0.00

The number of undergraduates funded by this agreement who graduated during this period with a degree in science, mathematics, engineering, or technology fields:..... 0.00

The number of undergraduates funded by your agreement who graduated during this period and will continue to pursue a graduate or Ph.D. degree in science, mathematics, engineering, or technology fields:..... 0.00

Number of graduating undergraduates who achieved a 3.5 GPA to 4.0 (4.0 max scale):..... 0.00

Number of graduating undergraduates funded by a DoD funded Center of Excellence grant for Education, Research and Engineering:..... 0.00

The number of undergraduates funded by your agreement who graduated during this period and intend to work for the Department of Defense 0.00

The number of undergraduates funded by your agreement who graduated during this period and will receive scholarships or fellowships for further studies in science, mathematics, engineering or technology fields: 0.00

Names of Personnel receiving masters degrees

NAME

Total Number:

Names of personnel receiving PHDs

NAME

Total Number:

Names of other research staff

NAME

PERCENT SUPPORTED

FTE Equivalent:

Total Number:

Sub Contractors (DD882)

Inventions (DD882)

Scientific Progress

Technology Transfer

Foreword

The primary objective of the proposed project is to investigate the effects of any seawater degradation of Carbon Fiber Reinforced Polymer (CFRP) and Glass Fiber Reinforced Polymer (GFRP) composite panels on the compressive strength after impact. Durability and dynamic failure properties are critical parameters for naval composite ships in seawater. However, previous approaches and measurements have significantly underestimated the actual durability of a composite structure inside seawater. A primary mode of failure of such composite panels is the compressional failure where the composite microstructure has been compromised by damage, typically due to impact. These failures are historically seen as being driven by the properties of the matrix and the adhesion of the matrix to the fiber.

Table of Contents

Foreword.....	1
Table of Contents.....	Error! Bookmark not defined.
Statement of the problem studied	1
Summary of the most important results	2
3.1 Material exposure experiments and CAI Testing.....	2
3.3 Notch-interface failure criteria	7
Conclusions	10
Bibliography	10

Statement of the problem studied

Durability and dynamic failure properties are critical parameters for naval composite ships in seawater. However, previous approaches and measurements have significantly underestimated the actual durability of a composite structure inside seawater. For a composite ship, a rectangular composite specimen only represents a part of an “infinite” large panel, and has one external face exposed to seawater. During underwater explosion, this front surface is subjected to shock loading first. For the whole life cycle of a composite ship, since only the front surface of a composite panel is directly exposed to seawater, property degradation and damage from the front surface will be a major issue to determine the durability and life of the composite ship structure. However, almost all previous experiments ignored this “single-surface environment effect”. For example, Karasek et al. (1995) have evaluated the influence of temperature and moisture on the impact resistance of epoxy/graphite fiber composites. They found that only at elevated temperatures, moisture had a significant effect on damage initiation energy and that the energy required to initiate damage was found to decrease with temperature. Impact damage resistance and tolerance of two high performance polymeric systems was studied after exposure to environmental aging. For cross-ply laminates, the post-impact tensile strength values fell significantly (by maximum 70–75% of original composite strength) depending on aging time, environment and impact velocity. Sala (2000) found that barely visible impact damage, due to the impact of 1 J/mm (for 2.2-mm laminate thickness) increased the moisture saturation level from 4.8% to

6% for aramid fiber-reinforced laminates and enhanced the absorption rate. Very recently, Imielinska and Guillaumat (2004) investigated two different woven glass–aramid-fiber/epoxy laminates subjected to water immersion aging followed by instrumented low velocity impact testing. The impacted plates were retested statically in compression to determine residual strength for assessment of damage tolerance. The delamination threshold load and impact energy absorption were not significantly affected by the absorbed water. Due to low fiber–matrix adhesion, the prevailing failure modes at low impact energy were fiber/matrix debonding and interfacial cracking. The compression strength suffered significant reductions with water absorbed (28%) and impact (maximum 42%). In addition to impact experiments, other mechanical experiments related to seawater durability also reported similar approaches using fully immersed composite specimens (Smith and Weitsman, 1996; Strait et al., 1992; Wood and Bradley, 1997; Weitsman and Elahi, 2000). In these previous specimens, property degradation such as matrix cracks in two vertical edges occurred, while these cracks never had the chance to initiate in a closed-edge, “infinite large” composite ship hull. Therefore, the previous data significantly underestimated the actual durability of composite structures inside seawater. In this project, our “composite fish tank” will provide more accurate measurements for composite durability.

Summary of the most important results

For this performance period the primary effort was in

- 1) Closing out the CAI impact experiments and
- 2) Developing the notch-failure criteria

The progress on the proposed tasks is detailed in the subsequent paragraphs.

3.1 Material exposure experiments and CAI Testing

Materials and Sample Preparation - The glass fiber reinforced vinyl ester (Glass/VE) and carbon fiber reinforced vinyl ester (Carbon/VE) were produced using a vacuum assisted resin transfer molding (VARTM) (Pillay 2001). Eight layers of plain weave fabric (CWR 2400/50 plain, UAB) were used to produce the panels with an average thickness of 5 mm as required by ASTM D 7137 “Standard Test Method for Compressive Residual Strength Properties of Damaged Polymer Matrix Composite Plates”. Compression after impact (CAI) testing samples with dimension 101.6 mm x 152.4 mm (4” x 6”) were cut and machine to meet the dimensions requirement specified in ASTM D 7137. In addition to, samples with the dimensions of 152.4 mm x 25.4 mm (6” x 1”) were cut to perform tension after impact (TAI) testing.

Seawater experiments using real and composite fish tanks - In order to simulate one-surface seawater absorption, silicone rubber as aquarium sealant (Perfecto Manufacturing, Noblesville, IN) was applied to four slots of a base PMMA plate before four composite specimens were inserted. PMMA has very little reaction with seawater. The reason to use silicone rubber is that it provides enough bonding strength under water pressure, at the same time, it is not too strong to break down the tank for future impact experiments. After one week of the construction of this tank (full bonding strength), it was filled with synthetic seawater (Ricca Chemical Co., TX). This tank will be disassembled after certain periods of time such as three months, six months etc. to conduct impact and compression experiments (Xu et al., 2012). The impact experiments of dry specimens were conducted to provide baseline data for future durability experiments.

Meanwhile, PMMA strips with the dimension of 12.7 mm x 228.6 mm x 6.35 mm (0.5" x 9" x 0.25") were placed in a 20-gallon fish tank such that six specimens could lay flat onto them (nickname "real fish tank"). A silicone rubber was used to ensure that the PMMA plates bond to the 20-gallon fish tank. The TAI testing samples were bonded sided by side in sets of 4 to form a plate with the same dimensions of the CAI testing samples. The silicone rubber was put on the edges of the CAI testing samples and TAI bundles so that seawater would not seep through the edges. In addition to the real fish tank, a composite seawater tank was made with silicone rubber as an aquarium sealant which was applied to the four slots of a base PMMA plate to bond the four composites specimens in the form of a small seawater tank (nickname "composite fish tank"). The sealant was also applied to the sides of the composite specimens to prevent any leakage of seawater. PMMA was chosen as the material for the base plate as it has little chemical reaction with seawater. Silicone rubber is used as a preferred sealant over other adhesives as it provides enough bonding strength bonding strength under water pressure, while at the same time is not too strong to cause significant damage in the composite samples when the tank structure is disassembled for impact experiments.

Once the construction of the tanks was completed (after full bonding strength of silicone rubber is achieved), the tanks were filled with synthetic seawater (Abilene, TX). Artificial seawater has a salinity content of 2.9% and has a variety of salt constituents according to ASTM D1141. The synthetic seawater is replaced at regular intervals of time and the water level inside each tank is maintained throughout the testing period. Impact experiments were conducted on the dry specimens at first to determine baseline properties. The either compression or tensile testing was conducted to characterize the residual strength after impact.

The composites were also withdrawn from the seawater at regular intervals, wiped dry to remove surface moisture, and then weighed to within an accuracy of 1 mg to monitor the mass change behavior. The percentage mass change of the composite panel (M) can be calculated by the simple expression:

$$M = \frac{M_t - M_o}{M_o} \times 100, \quad (1)$$

where M_t is the mass of the panel after a given immersion time and M_o is the original panel mass.

It is important to note that only one face of the composite specimen was exposed to the seawater similar as would be seen in naval ships. Furthermore, the face exposed to seawater did not have a gel coat which normally protect the marine composite.

Moisture absorption process in EVE and other polymer matrix composites is typically idealized using Fick's second law of diffusion. Murthy et al provides the coefficients of diffusions at room temperature, D , for an identical construction of EVE composite.

Impact experiments of durability specimens - Impact damage was introduced using a drop tower setup. All samples (fixed four edges) were subjected to an impact using a hemispherical impactor. The CAI specimens were subjected to a 60 joule impact energy while the TAI specimens were subjected to a 20 joule impact energy. For the front surface directly subjected to impact, dark areas represent internal delamination, with possible several delaminations at the different interfaces. As discussed by Xu and Rosakis (2002), these delaminations are mainly shear-dominated so the interlaminar shear strength is an important parameter for delamination resistance characterization. Also, two major matrix cracks were observed near the impact site. One matrix crack was along the horizontal direction and the other one

was along the vertical direction. On the back surface of the impacted specimen, fiber breakage was observed at the impact site and this failure mode contributed to major impact energy absorption. Meanwhile, fiber/matrix debonding appeared as white thin lines on the back surface of the impacted specimens. These four major failure modes indeed make different contributions to the composite impact resistance (Abrate, 1998), and we believe fiber breakage and delamination play the major role to absorb impact energy.

Compression-after-impact strength as an index to combine seawater and impact effects - Impacted samples were mounted into a compression fixture. A loading rate of 1 mm/min was used. The progressive compression failure started from the impact damage. Initially, as the compression load increased, delamination from the previous impact propagated in a local buckling form. Unlike impact-induced delamination, its propagation is mainly opening-dominated. Notice that delamination also appeared along the horizontal matrix crack and this matrix crack extended to the two edges as the compressive loading increased. The final failure (maximum load) was controlled by a shear crack near the horizontal matrix crack. An inclined angle around 30-45 degrees (with respect to the compressive loading direction) was observed from the two vertical edges of the failed specimen. These results are similar to previous compressive failure results by Daniel and Ishai (2006), Tsai and Sun (2004), Oguni and Ravichandran (2001). From load-displacement curve for a compressive experiment of an impacted specimen, the initial non-linear part is caused by the initial gap of the compressive fixture. Then a long linear load-displacement part was recorded. The failure mode starts from the opening delamination from the impacted-induced delamination (shear-dominated), followed by a sudden propagation of the longitudinal matrix crack and a final shear crack appeared along the specimen edge based on the recorded high-definition video. The CAI strength of dry composite specimens was used as a baseline for comparison. Since the CAI strength combines the effects of the seawater exposure and impact damage, it is very convenient to be used as an evaluation parameter. We notice that the CAI strength reduction is almost 0% after two-month seawater exposure. Therefore, we need at least one-year seawater exposure to observe some CAI strength reduction.

Tension-after-Impact strength as an index to combine seawater and impact effects- Impact TAI samples were mounted onto an Instron fatigue machine such that the grips held each side 45 mm from the center of the impact. A loading rate of 1 mm/min was used. Similar to compression, the progressive tensile failure started from the impact damage. As the tensile load increased, delamination began to propagate along the plane of the load. The final failure (maximum) load was controlled by a normal crack near the horizontal matrix. Then a long linear load-displacement curve for a tensile experiment was recorded. The failure mode starts from the opening of the delamination from the impacted-induced delamination, followed by a slow propagation along the loading direction until ultimate failure of the matrix. The TAI strength of the dry composite specimens was used as a baseline for comparison. Since the TAI strength combines the effects of the seawater exposure and impact damage, it is very convenient to be used as an evaluation parameter. Therefore we need at least one-year seawater exposure to be observed some TAI strength reduction.

Seawater Absorption - The seawater absorption, which is the percentage mass change of the glass/vinyl ester and carbon/vinyl ester composites, is shown in Figure 1. Both composites have the same vinyl ester matrix content and were prepared using the same VARTM method. The respective average thickness for the GFRP and the CFRP were 4.75 mm and 5.01 mm all through the immersion time. The profiles for the uptake of seawater are similar as immersion time increases. The seawater absorption

content increased rapidly when the composites were immersed in seawater until the 120th day where both composites reached saturation. The carbon/vinyl ester composites seawater moisture began to saturate at 0.2% while the glass/vinyl ester began to saturate at 0.14%.

While the mass change curves for the two vinyl ester based composites show the same profile with increasing immersion time, the mass gain is higher for the carbon composite. Both materials have similar resin content, and therefore the higher mass gain cannot be due to greater seawater absorption by the vinyl ester matrix. In previous studies, glass fibers are known to chemically react with water. However, in this study it would appear the carbon fibers might absorb seawater more than glass fibers. The difference may be due to the greater amount of moisture absorption at the carbon/vinyl ester interphase region than the glass/vinyl ester interphase region.

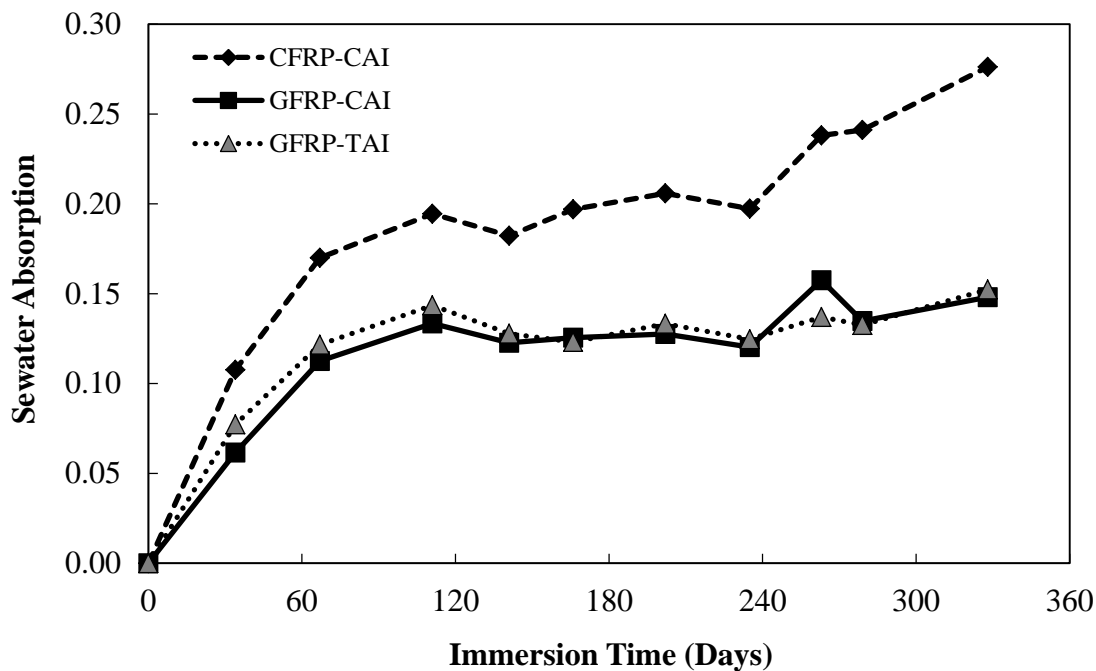


Figure 1 – Seawater Absorption vs Immersion Time

Effects of Seawater Uptake on Compression After Impact Strength - Figure 2 shows the compression after impact strength of the glass and carbon fiber composites with their respective baseline strength. Though all the specimens show a drop in CAI strength after 300 days of immersion time, carbon fiber reinforced polymers had lower values in strength. Peculiar events occurred with the GFRP. Even though there was a sharp decrease in compression strength after 30 days, it began to recover some of its strength after 138 days. By the 323rd day, the GFRP compression strength dropped by 19.4% from the baseline strength. For the CFRP, the CAI strength began to increase and by the 162nd day began to decrease from the baseline strength. By the 324th day, the CFRP CAI dropped 19.9% from the baseline strength.

The difference in compression strength could be attributed to a mismatch between the mechanical properties of the fiber and matrix. Since the carbon fiber's modulus is significantly higher than that of

glass, the interface region may carry different damage. There was also a slight difference of thickness between the carbon and glass. The carbon average thickness was 5 mm while the glass composite was 4.75 mm. Over all they both showed degradation in orders of the same magnitude.

Both of the curves have not shown that their properties degrade by Fick's law of diffusion with respect to seawater uptake. There is no stabilization of the CAI that can be concluded after a years worth of experiments.

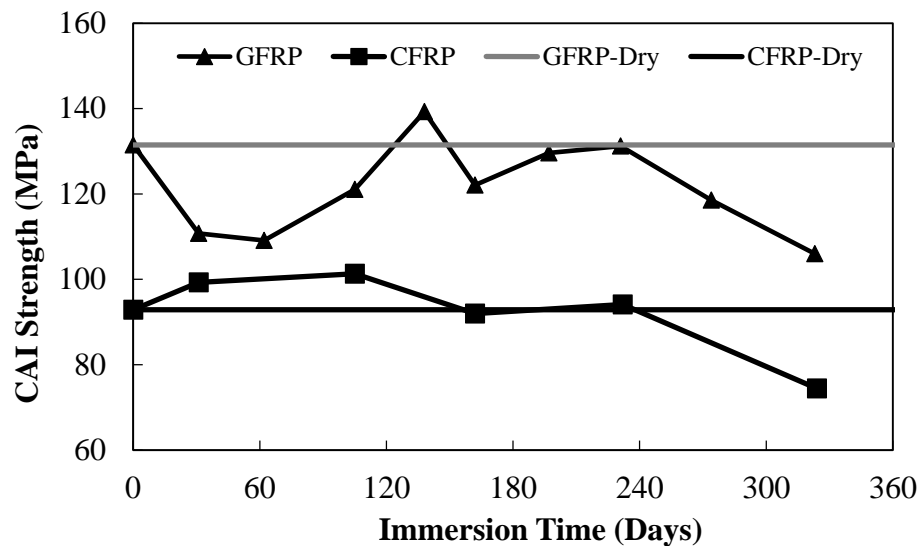


Figure 2 – Compression Strength vs Immersion Time

Effects of Seawater Uptake for Tension After Impact Strength - The behavior of vinyl ester/glass composites was observed to be similar to tests conducted by others. The degradation of the tensile conformed to Fick's law of diffusion as the strength began to stabilize after a 180-day period. However, since the specimens were not cut into dog bones specimens to conform to tensile loadings, the failure of the composites began to occur are the grip of the fatigue machine. The complexity of the failure was different for each specimen and would propagate in the direction of the loading. After 323 days of immersion time, the strength dropped by 20% of the baseline strength. After 323 days, specimens that were kept under room temperature at 10 C were tested and specimen's strength dropped by 6% from the baseline strength.

The difference between the cold and room temperature specimens could be attributed to the conditions they were put into. Arid conditions caused the seawater to evaporate at different levels than would at room temperature. Water levels in the refrigerator had to be maintained twice the amount as the room temperature specimens.

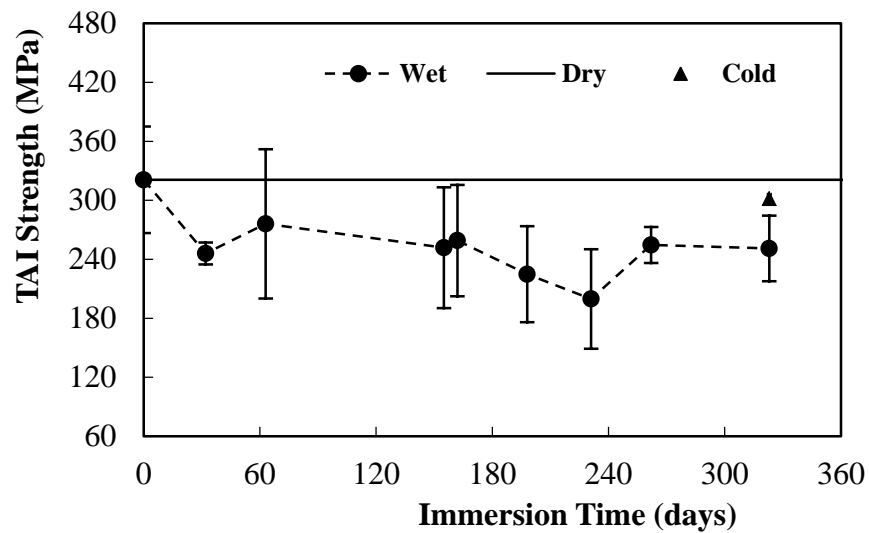


Figure 3 – TAI Strength vs Immersion Time

3.3 Notch-interface failure criteria

The work on this task was just started in the end of the performance period. The notched bi-material shear specimens were fabricated and will be conducted at Wright Patterson Air Force Base in the summer and fall of 2013 as well as at UTEP. Some of the specimens will be tested using the Digital Image Correlation (DIC) apparatus as WPAFB to validate the FEA and testing results at UTEP. Results will be reported in the final report for this project.

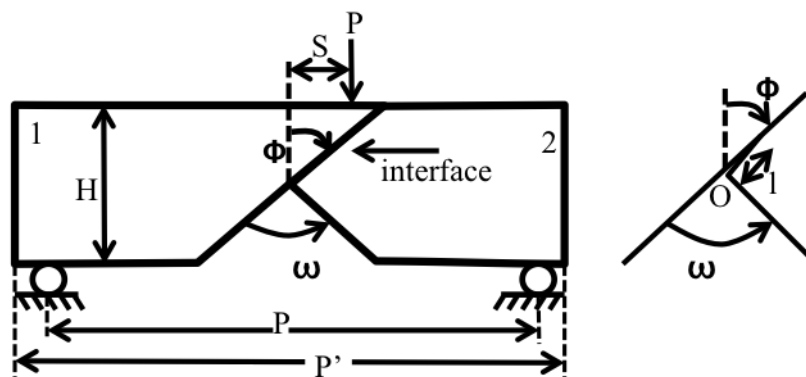


Figure 4 Proposed Notch Experiment Geometry.

Figure 5 shows a preliminary DIC visualization of the notch specimen undergoing shear

loading. This was performed at WPAFB by Mr. Mark Flores, one of the students supported by this project.

In order to study the mechanical behavior of the V-notch for bonded dissimilar materials, Iosipescu shear method is adopted for testing. Aluminum and Polycarbonate are the materials we used to bond V-

notch. Each specimen contains two parts which are aluminum and PMMA bonded with Loctite Super Glue Gel Control. The bonding strength will be relatively low if we use weak adhesive because of small bonding area. This will result in early failure before we can record enough data. Every specimen was bonded together from separate halves to enable an interfacial failure and all of the individual bonding surfaces were sanded. Prior to bonding, plastics and aluminum were cleaned and degreased by alcohol and acetone respectively in order to improve the bonding quality. The specimens were cured for a period of 24 hours before removed from the fixture in order to achieve the bonding strength under room temperature. A schematic diagram of V-notch specimen loaded in Iosipescu shear fixture is shown in Fig. 1. Experiments are conducted by hydraulically driven material test machine (Instron 8100) with a loading rate of 1 mm/min. Nine groups of V-notch specimens with included angle of 5, 10, 15, 20, 25, 30, 40, 50 and 60 degrees are tested.

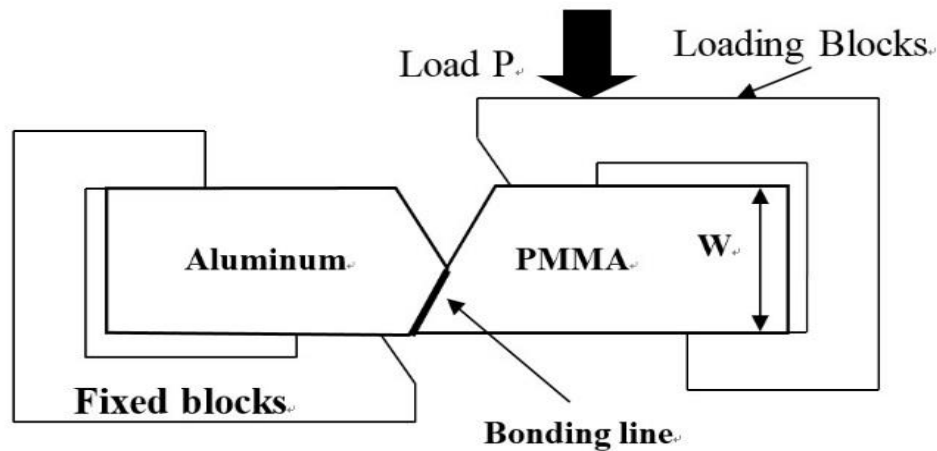


Fig. 5 Schematic diagram of V-notch specimen loaded in Iosipescu shear fixture

4. FINITE ELEMENT ANALYSIS

A two-dimensional finite element analysis was conducted using Abaqus® 6.10.1. The Iosipescu shear fixture is modeled as rigid body. Right part of the fixture is fixed while the left applies displacement. The fixture and specimen are modeled as surface-to-surface contact. Cohesive elements are used to define the bonding between aluminum and Polycarbonate in order to simulate the experimental load-displacement curves and the failure load. The loading is applied in the form of loading block on the specimen edges similar to what is observed in reality. In order to incorporate a realistic simulation of the loads on the specimen, a contact model is adopted. The loads in the form of displacements are applied to the movable part of the specimen while the other part is held fixed.

As showing in Fig. 2 and Fig. 3, the FEA simulation predicts crack initiation load very well. Five different experimental curves are shown to depict the variation in the experiments.

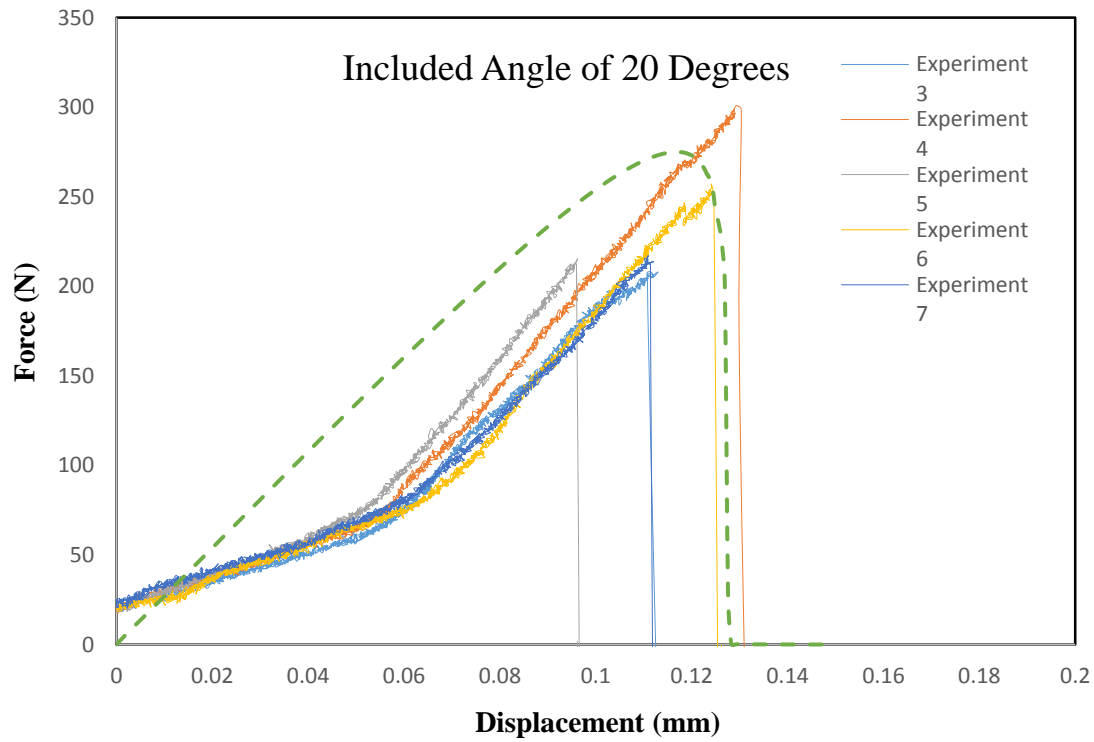


Fig. 6. Comparison of Load – Displacement Curve between Experiments and FEA (20 Degrees)

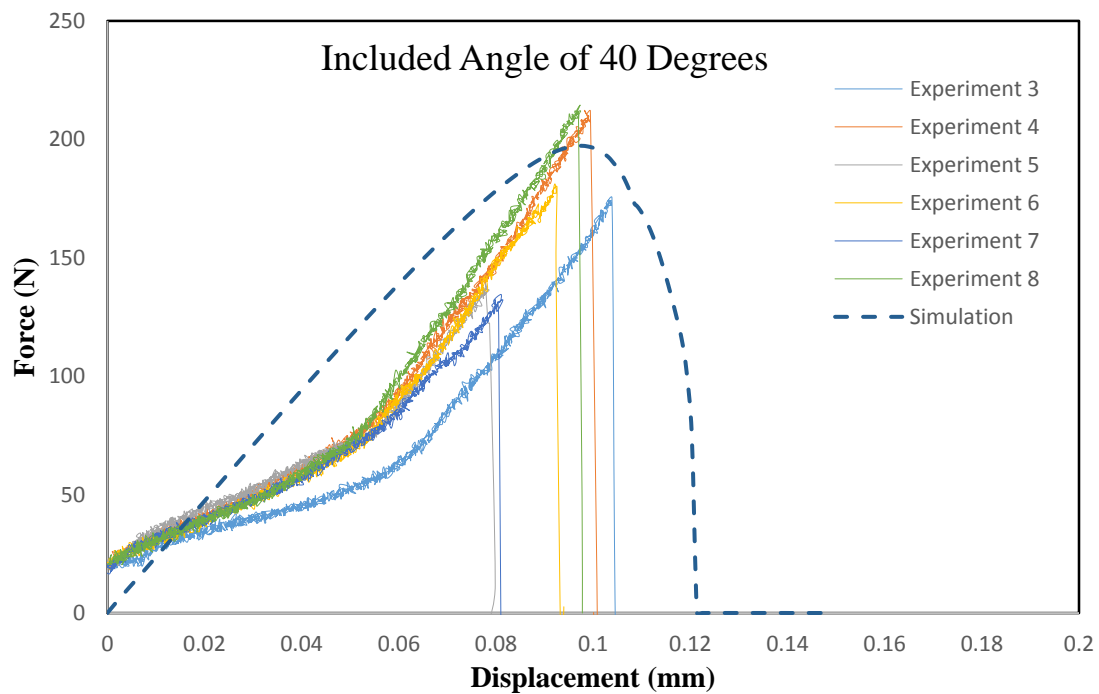


Fig. 7. Comparison of Load – Displacement Curve between Experiments and FEA (40 Degrees)

Conclusions

With respect to the CAI and water absorption work there seems to be a very slight suggestion of the swelling effect causing a transient strength enhancement at about the 6 month time frame. A potential mechanism is that the swelling builds a residual stress that resists the micro buckling and kink banding formation during the compression tests. But, when viewed in the light of statistical analysis this seems somewhat of a dubious claim. But the major conclusion should be that there is not significant degradation of these composite systems, both the carbon and glass fiber systems with prolonged exposure to seawater. The swelling strength enhancement does seem as if something to pursue.

The notch-failure criterion was shown not to be a promising approach. While we were able to fit appropriate cohesive models the fitting of the generalized stress intensity factor was not able to capture the complexity of the stress decay and the multi-modality of the bi-material notched interface. In the opinion of the researchers this approach, while academically appealing, is not viable in a “real world” composite damage scenario. The actual damage topology seen after the impact damage on a weave is fundamentally different than that idealized in the proposed notch analog in Figure 5.

Bibliography

- A. Krishnan and C. Oskay, Modeling compression-after-impact response of polymer matrix composites subjected to seawater aging, *Journal of Composite Materials*.
1. K. Woo and J. Whitcomb, A post-processor approach for stress analysis of woven textile composites, *Composite Sciences, and Technology* 60 (2000) 693-704
2. J. Hutchinson and H. Jensen, Models of fiber debonding and pullout in brittle composite with friction, *Mechanics of Materials* 9 (1990) 139-163
3. Abrate, S., (1998). *Impact on composite structures*, Cambridge University Press, New York.
4. Daniel IM, Ishai O (2006). *Engineering Mechanics of Composite Materials*. Oxford University Press, New York.
5. Fisher-Cripps AC (2004). *Nano-indentation*, Springer, New York.
6. Giannakopoulos, A.E., Suresh, S., (1999). Determination of elastoplastic properties by instrumented sharp indentation. *Scripta Materialia*. 40, 1191–1198.
7. Hutchinson J, Suo Z. (1992) Mixed-mode cracking in layered materials, *Advances in Applied Mechanics* 29, 63-191.
8. Imielinska, K. and Guillaumat, L. , (2004). The effect of water immersion ageing on low-velocity impact behaviour of woven aramid–glass fibre/epoxy composites, *Composite Science and Technology*, 64, 2271–2278.
9. Karasek, M.C., Strait, L.H., and Amateau, M.F., (1995). Effect of temperature and moisture on the impact behaviour of graphite/epoxy composites: parts I and II. *Journal of Material Res Technol* 17(1), 3–15.
10. Krishnan A. and L. R. Xu, (2012). A Simple Effective Flaw Model on Analyzing the Nanofiller Agglomeration Effect of Nanocomposite Materials,” *Journal of Nanomaterials*, DOI:10.1155/2012/483093.
11. Leguillon D., (2002). Strength or toughness? A criterion for crack onset at a notch. *European Journal of Mechanics A/Solids* 21, 61-72.

12. Oliver WC, Pharr GM (1992). An improved technique for determining hardness and elastic modulus using load and displacement sensing indentation experiments. *Journal of Material Res.* 7: 1564-1582.
13. Oguni, K., and Ravichandran, G., (2001). Dynamic compressive behavior of unidirectional E-glass/vinylester composites. *Journal of Materials Science*, 36, 831-838.
14. Pillay, S., Vaidya U.K., and Janowski, G.M., (2005). Liquid molding of carbon fabric-reinforced nylon matrix composite laminates. *Journal of Thermoplastic Composite Materials*, 18, 509-527.
15. Sala, G., (2000). Composite degradation to fluid absorption. *Composites Part B* 31, 357-377.
16. Smith, L.V., and Weitsman, Y. J., (1996). The immersed fatigue response of polymer composites, *International Journal of Fracture*, 82, 31-42.
17. Strait, L.H., Karasek, M.L. and Amateau, M.F., (1992). Effects of seawater immersion on the impact resistance of glass fiber reinforced epoxy composites, *Journal of Composite Materials*, 26, 2118- 2133.
18. Tran V.-X. , D. Leguillon, A. Krishnan and L. R. Xu (2012). Interface Crack Initiation at V-Notches along Adhesive Bonding in Weakly Bonded Polymers Subjected to Mixed-Mode Loading,” *International Journal of Fracture*, 176, 65-79.
19. Tsai, J. and Sun, C.T., (2004), Dynamic compressive strength of polymeric composites, *International Journal of Solids and Structures*, 41, 3211-3224.
20. Ulven, C., and Vaidya, U. K., (2006). Post-fire low velocity impact response of marine grade sandwich composites. *Composites Part A*, 37, 997-1004.
21. Weitsman, Y.J., and Elahi, M., (2000). Effects of fluids on the deformation, strength and durability of polymeric composites—an overview. *Mechanical Time- Dependent Materials*, 4,107–126.
22. Williams ML. (1952). Stress singularities resulting from various boundary conditions in angular corners of plates in extension, *Journal of Applied Mechanics*, 19, 526-528.
23. Wood, C.A., and Bradley, W., (1997). Determination of the effect of seawater on the interfacial strength of an interlayer E-glass/graphite/epoxy composite by in situ observation of transverse cracking in an environmental SEM. *Composite Science and Technology*, 57, 1033-1045.
24. Willis JR (1996). Hertzian contact of anisotropic bodies. *Journal of Mechanics and Physics of Solids*, 14:163-176.
25. Xu, L. R. and Rosakis, A. J., (2002). Impact failure characteristics in sandwich structures; Part I: Basic Failure Mode Selections. *International Journal of Solids and Structures*, 39, 4215-4235.
26. Xu, L. R. and Arun Krishnan; Haibin Ning; Uday Vaidya, (2012). A seawater tank approach to evaluate the dynamic failure and durability of E-glass/vinyl ester marine composites, *Composites Part B.* 43, [2480–2486](#),
27. Yang SH, Sun CT (1982). Indentation Law for Composite Laminates. *ASTM STP*, pp. 425-449.